JOURNAL OF ENGINEERING AND TECHNOLOGY (JET), VOL.6 NO.1&2, pp.48-55.

PREDICTING STEADY-STATE CHARACTERISTICS (OR RESPONSE) OF INDUCTION MOTOR USING FINITE ELEMENTS

IBRAHIM, S.B.

Department of Electrical Engineering, Bayero University, Kano

ABSTRACT

A method for predicting the steady-state performance of a squirrel-cage induction motor using finite element models was described.The method was used in conjunction with the conventional equivalent circuit model for a three-phase induction motor. The method uses separate finite element models for the rotor and the stator consisting of one slot pitch and one phase band, respectively. The use of minimal models led to a fast execution time for the finite element analysis.The method is illustrated by comparing finite element model predictions of performance with test measurements made on a 4-pole, 4 kW induction motor which shows a very good correlation.

KEYWORDS: steady-state, finite element, induction motor.

1. INTRODUCTION

Traditionally, electrical machines parameters have been evaluated from formulae based on approximations to actual flux distribution in the machine. Inacurracies in the performance prediction, resulting from these approximations, make it necessary to employ improved analytical models (Tandon *et al.,* 1980). With the advent of modern digital computers, numerical methods have become practical and are being used to improve the accuracy of magnetic field computations. The Finite elements method (Zienkiewicz and Cheung, 1967) has emerged as a useful numerical method for solving a wide class of distributed problems that arise in mathematical physics. Indeed, the finite element method has been used with considerable success in the areas of electrical machines design, structural mechanics, fluid flow, and heat conduction.

The main disadvantage of the use of Finite elements in machine analysis is that it usually involves the use of prodigious amount of computer resources. It is therefore, important to choose a model that is well suited to the task in hand. A model that is developed for steady-state performance prediction may not be appropropriate for transient analysis. Whereas a transient model is unnecessary expensive for a steady-state performance analysis (Williamson *et al.,* 1990). The steady-state performance of an induction motor is classically evaluated using an equivalent circuit (Williamson et al., 1986). A standard three-phase cage induction motor exhibits a greater degree of symmetry, facilitating the exploitation of that symmetry to produce an effective steady-state model of the machine.

This paper describes the application of the finite element method for the field solution aspects of the steady-state model.

2. THEORETICAL FUNDAMENTALS

2.1 Nonlinear Magnetic Field Analysis of Induction Motor Cross Section

The basic problem of the flux (field) distribution in the cross-section of a cage induction motor is solved by the following elliptic equation:

$$\frac{\partial}{\partial x}\bullet\nu\left[\frac{\partial A_Z}{\partial x}\right]+\frac{\partial}{\partial y}\bullet\nu\left[\frac{\partial A_Z}{\partial y}\right]=-J_Z \quad ..(1)$$

Where: ν - is the reluctivity of the region (assumed constant for a given region); A_Z - is the magnetic vector potential normal to the section;

J_Z - is the current density vector normal to the section; *x* and *y* - are the Cartesian coordinates.

This equation is reformulated by variational calculus, and first-order triangular elements are used to discretize the field region, resulting in a set of linear algebraic equations. These linear simultaneous equations are solved using Gaussian elimination techniques.

2.2 Steady-State Analysis

The primary function of steady-state analysis of induction motors is to predict performance during design synthesis or analysis. In essence, the designer uses relatively simple design rules to produce a design and then carries out a prediction analysis to compute its performance. If the computed performance meets the required specification, the design may be deemed satisfactory; otherwise adjustments are made and the performance recomputed. Clearly the analysis method must be both quick and accurate. Speed is essential if a number of design amendments must be made or a number of alternatives assessed.

Accuracy is important to ensure that the machine performance is reliably predicted, so that margins for error can be reduced without increasing the risk of expensive post-manufacture modifications. To a large extent, these two requirements are in direct contradiction. Greater accuracy inevitably implies an increasingly complex model, which in turn implies an increase in computing time. It is therefore important that a compromise solution be adopted giving "improved" accuracy subject to "reasonable" computing time. Classical induction motor analysis is based on the familiar steady-state per phase equivalent circuit (Figure 1).

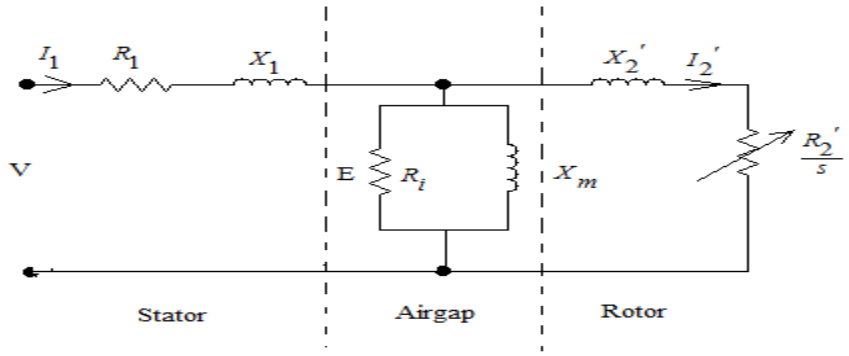

Figure1: Per Phase Equivalent Circuit.

As seen in Figure 1, R_1 - denotes the stator resistance per phase; X_1 - denotes the stator reactance per phase; R_i - denotes the equivalence of the core losses associated with the motor; X_m - denotes the mutual reactance; X_2 - denotes the rotor reactance per phase and X_2' - the electrical equivalent of the mechanical load on the motor. A feature of this model is that it consists of parts that may be attributed to the stator, the rotor, and the air-gap as shown in Figure 1. For the purposes of developing a finite element-based analysis, this feature is most attractive because it enables the field models for the stator and rotor to be decoupled, so that minimal models may be used for each.

3.0 MATERIALS AND METHODS

The basis of the method used in this paper, involves the following sequence of steps:

Step 1: Calculation of the equivalent-circuit components by any convenient means, and solve to determine the first estimates of stator and rotor current.

Step 2: Use the most recent estimates of stator and rotor current as field sources in a separate finite element field model. Calculate new

values of the equivalent circuit components from the resulting field solutions.

Step 3: Resolve the equivalent circuit model using the latest values for the equivalent circuit components. Compare the new estimates of the currents with the previous values and check for convergence. If convergence is satisfactory, calculate input power, torque etc from the equivalent circuit model; if it is not, go to step 2.

The described procedure is dependent on the use of finite element models for the rotor and stator.

3.1 Rotor Model

It consists of a sector of the rotor corresponding to one rotor slot pitch (Figure 2). The presence of the rest of the rotor of the motor is implied in the model by means of an appropriate periodic boundary condition, specified along the radial boundaries.

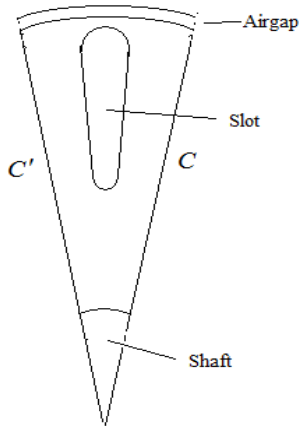

Figure 2: Rotor Model Used for Steady-State Analysis

The vector potential at corresponding boundary nodes C and C' as shown in Fig. 2 is related by the equation:

$$A_{C'} = A_C e^{-j\alpha} \quad \ldots \quad (2)$$

Where: α - is the rotor slot pitch.

The inner most circumferential boundary represents the interface of the rotor core with the shaft. The penetration of the rotor flux into the shaft is largely a function of the rotor frequency. At the instant of starting the motor, the rotor currents have same frequency as the supply frequency (i.e., f = 50Hz) and the shaft is almost impervious to flux. When the motor is on no-load the rotor currents have very low frequency (i.e., a frequency = slip times frequency) and the shaft may carry a significant proportion of the rotor core-back flux.

For all other conditions of the motor, the flux entering the shaft can be neglected, and the inner circumferential boundary of the rotor then becomes a flux line (i.e., A = 0).

The model also includes part of the airgap, corresponding to one rotor slot pitch, and the outer circumferential boundary therefore represents the inside surface of the stator. As stator iron saturation is not included in the rotor model, this surface is represented by an infinitely permeable boundary. The rotor model gives an accurate representation of the rotor slot but does not model the stator slotting. The radial length of the airgap used in this model is therefore equal to the physical airgap length multiplied by Carter's coefficient for the stator.

The rotor model used to determine the rotor leakage reactance, X_2 and resistance R_2 for a specified rotor bar current. The distribution of the rotor bar current depends on both frequency and the bar shape. A suitable formulation was proposed by (Konrad, 1981), showing that the appropriate governing field equation to be solved should account for the redistribution of the current due to skin effect:

$$\nabla \bullet \nu \ \nabla A = -J_o + j\omega\sigma\left(A - A_o\right) \quad \ldots (3)$$

Where: σ - is the electric conductivity; J_o - is the space-average (or low frequency) value of the bar current density; and A_o - is the space-average value of the magnetic vector potential over the bar cross-section.

The same equation is employed throughout the rotor model with suitable selection of the terms on the right hand side (i.e., $J_o = 0, \quad \sigma = 0$ for the airgap, $J_o = 0, \quad A_o = 0$ for the rotor shaft, and so forth). Saturation in the rotor depends on both the rotor and stator MMFs, and it is therefore necessary to include the stator MMF in the rotor model. This is achieved by means of a thin current sheet placed on the inside surface of the stator. The required current density, J_s was initially estimated from the latest estimates of the rotor bar impedance, Z_b as in Williamson and Begg (1985, 1986).

$$J_s = -\left[\frac{I_b}{\pi d}\right]\left(N_b - \frac{4jp^2 g\pi}{\mu_o \omega d W} Z_b\right) \quad \ldots (4)$$

Where: I_b - the bar current; N_b - the number of rotor bars; p - is the number of pole pairs; ω - is the angular frequency; μ_o - is the permeability; d - is the mean diameter of the airgap; g - is the airgap length; and W - is the effective core length.

The field problem is then solved in a nonlinear sense (i.e., allowing reluctivity, ν to vary in the iron elements). When solution is obtained, a new estimate of the bar impedance is calculated by carrying out a linear field solution with only the bar current present and the reluctivities frozen at the values obtained at the end of the nonlinear solution.

The bar resistance is evaluated by calulating the joule loss in the bar (Williamson and Begg, 1985) and the bar leakage reactance by subtracting the magnetizing inductance from the total bar inductance. The bar impedance is then augmented by the end-ring resistance and leakage reactance which are calculated by classical means.

A check is then made, so that the flux density in the airgap, calculated during the nonlinear solution is sufficient to support the bar impedance drop $\left(I_b Z_b\right)$. If it is not, J_S is adjusted to the appropriate value and the procedure is repeated.

3.2 Stator Model

The symmetry that allows the use of a single slot model for the rotor does not extend to the stator. The teeth of the stator see different flux depending on their position in a phase band. These considerations led to the stator model to consist of one complete phase band as shown in Figure 3.

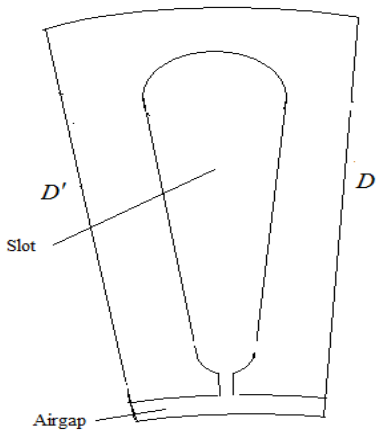

Figure 3: Stator Model Used for Steady-State Analysis

The phase band in a three-phase induction motor exhibits 60^o periodicity so that the vector potential relationship between the nodes D and D' as shown in Figure 3 is related as:

$$A_{D'} = A_D e^{-j\pi/3} \quad \ldots \quad (5)$$

The outer circumferential boundary represents the outer surface of the stator laminations, which is regarded as a flux line (i.e., core-back leakage flux is ignored). The inner boundary corresponds to the rotor surface, and the airgap length is set to the physical length multiplied by Carter's coefficient for the rotor. Skin effect in the stator conductors are neglected, so that it is assumed that the stator current density is distributed uniformly over the winding cross-section. The back-EMF, E as shown in Fig. 1 is calculated using the following equation:

$$V = I_1(R_1 + jX_1) + E \quad \ldots \quad (6)$$

Where: E - is calculated using equation (6) and the most recent estimates of the stator current, I_1 (from the equivalent circuit model) and stator leakage reactance X_1.

E is then used to determine the magnitude and space-phase of the flux wave needed to induce the back EMF, E. This in turn gives the required rotor surface current density distribution, I_b, via an iterative process (Williamson and Begg, 1985). The field problem is then solved in a nonlinear sense, with both stator current and rotor surface currents present. The value of the stator leakage reactance, X_1 so derived is augmented by the end-winding reactance, which again is calculated by classical means. The updated value of X_1 is substituted into equation (6) and the process repeated until X_1 converges to a constant value.

3.3 Airgap Model

From this model, the magnetizing reactance, X_m and iron loss resistance, R_i of the motor is determined. The stator iron losses are determined directly from the nonlinear field solution for the stator model. The magnetizing reactance of the motor varies because of saturation in both the stator and rotor. The use of separate models means that the stator and rotor are not simultaneously represented in any one field model, so that a means of separating out the effects of saturation for the stator and rotor parts of the iron circuit was obtained. The method used is based on the representation of magnetizing reactance by three parallel reactances as shown in Figure 4(a).

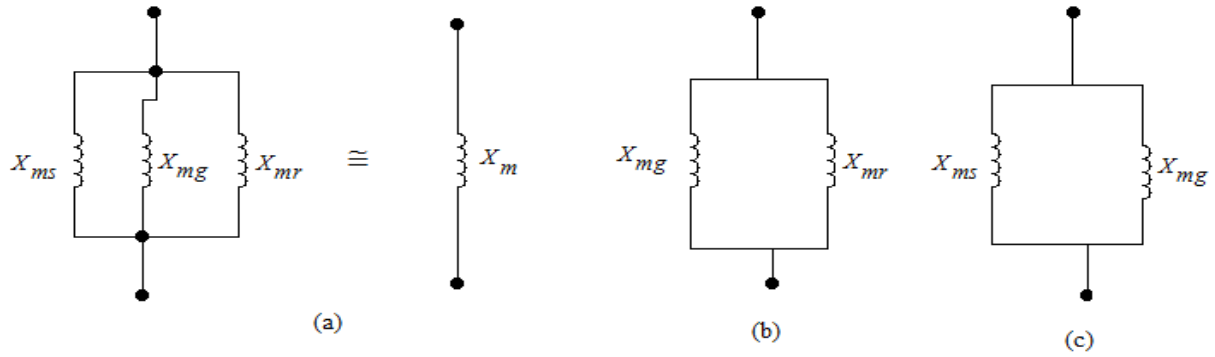

Figure 4: (a) Representation of Magnetizing Reactance for the Motor; (b) Representation with Rotor Only; (c) Representation with Stator Only.

X_{mg} is the component due to to the airgap, which is calculated using classical expressions assuming infinitely permeable iron. X_{mr} is a component that depends on the rotor iron saturation, and X_{ms} is the corresponding component depending on stator iron saturation. When the motor is unsaturated $X_{mr} = X_{ms} = \infty$, so that $X_m = X_{mg}$. As

saturation increases, X_{mr} and X_{ms} start to fall and therefore so does X_m.

When the rotor field model is being used, the stator iron is regarded as infinitely permeable, so that the magnetizing reactance becomes X_{mg} in parallel with X_{mr} as shown in Figure 4(b). The value of this parallel combination is obtained from the linear field solution by relating the bar current to the flux density. X_{mg} is obtained analytically, so that X_{mr} was calculated. Equally, when the stator field model is used, the rotor is regarded as infinitely permeable, so that the magnetizing reactance, X_m becomes X_{mg} in parallel with X_{ms} as shown in Figure 4(c). The stator model therefore allows X_{ms} to be obtained, and the three components in parallel give X_m.

4. RESULTS AND DISCUSSION

The method of analysis described has been verified by comparing test results with finite elements model predictions using a three- phase 415V, 4KW, 50Hz, 4-pole induction motor. The details of the motor are given in Table 1. Outlines of its stator and rotor slots are given in Figures 3 and 2 respectively. Experimental results were obtained with the test motor coupled in a Ward-Leonard speed control system via a rotating torque transducer. This enabled the speed of the motor to be held steady on the unstable part of the torque characteristics. Figure 5 compares the predicted no-load characteristics with that measured under test, while Figsures 6-8 compare part of the predicted load characteristics with measurement at rated line voltage of 415V.

.

Table 1: Details of 4kW Induction Motor

Power	**4KW**
Line Voltage	415V
Number of poles	4
Connection	Delta
Winding Type	Concentric
Mean airgap diameter	128mm
Airgap length	0.46mm
Lamination material	Newcor 800-65
Full load slip	0.0433
Gross core length	84mm
Number of stator slots	36
Number of turns/phase	342
Stator resistance (hot)	6.66 ohms
Number of rotor slots	28
Cage type	Cast Aluminium
Rotor conductivity (hot)	2.1×10^7
Rotor skew (rotor slot pitch	1

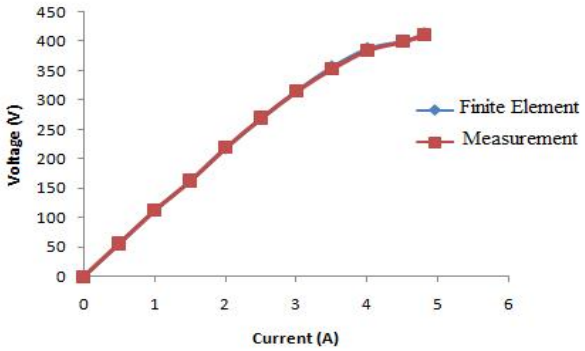

Fig. 5: No-Load Characteristics

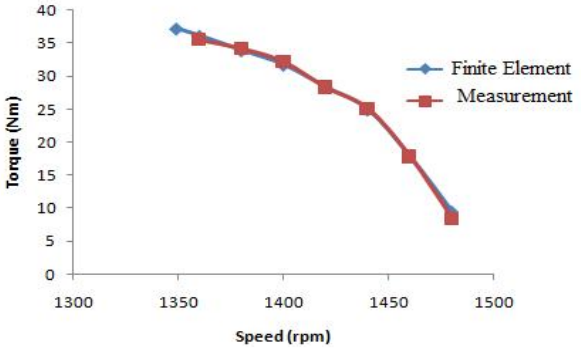

Fig. 6: Variation of Torque with Speed at Rated Voltage

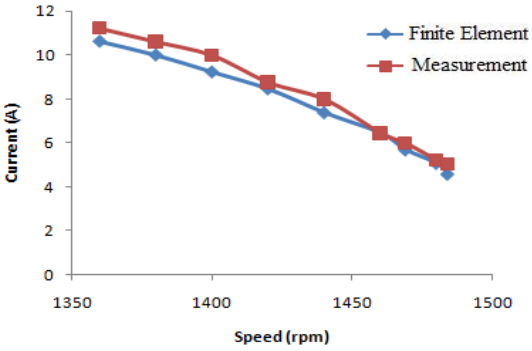

Fig. 7: Variation of Current with Speed at Rated Voltage

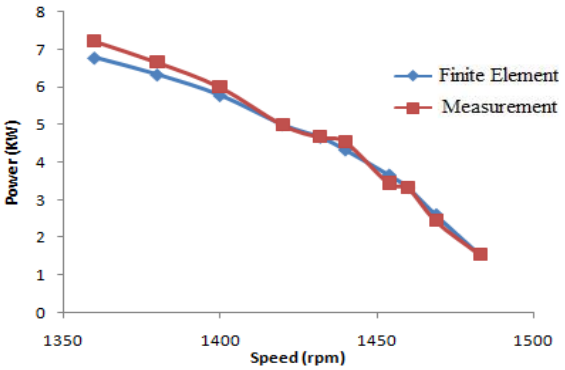

Fig. 8: Variation of Input Power with Speed at Rated Voltage

5. CONCLUSION

This paper outlined the method for conducting steady-state analysis of an induction motor using finite element models. The steady-state performance of an induction motor is classically evaluated using an equivalent circuit approach, which results in inaccurate predictions of the motor performance, however using FEM the performance of the machine can be accurately predicted as seen from the results of the analysis. The method uses separate finite element models for the rotor and the stator consisting of one slot pitch and one phase band, respectively. The use of minimal models led to a fast execution time for the finite element analysis. The method is based on the use of finite elements coupled to a circuit model of the motor. From Figure 5 there is a good correlation between the no-load characteristics prediction obtained from FEM and measurements conducted on the machine. Load test was carried out at rated voltage which led to a limited speed range of operation. To increase the range of speed over which the motor opeartes on-load will necessitate operating the motor at lower voltage level. The correlation between the finite element predictions and measurements is seen to be good.

REFERENCES

1. Konrad, A. (1981). "A numerical Solution of Steady-State Skin Effect Problems - An Integrodifferential Approach", IEEE Trans., Vol., MAG-17, No. 1, pp.1148-1152.
2. Tandon, S.C.; Richter, E.; and Chari, M.V.K (1980). "Finite Elements and Electrical Machine Design", IEEE Trans. on Magnetics, Vol. MAG-16, No. 5.
3. Williamson, S.; Lim, L.H.; and Robinson, M.J. (1990). "Finite Element Models for Cage Induction Motor Analysis", IEEE Trans. on Industry Applications, Vol., 26, No. 6, Nov/Dec,

4. Williamson, S.; Smith, A.C.; Begg, M.C.; and Smith, J.R. (1986). "General Techniques for the Analysis of Induction Machines Using Finite Elements", Conf. Record Int. Conf. on Evolution and Modern Aspects of Induction Machines, Turin, Italy, pp. 389-395.
5. Williamson, S. and Begg, M.C (1985). "Calculation of the Resistance and Leakage Reactance of Cage Rotors with Closed Slots", IEE Procs., Vol. 132, pt. B, No. 3, pp.125-132.
6. Williamson, S. and Begg, M.C. (1986). "Calculation of the Resistance of Induction Motor End-Rings", IEE Procs., Vol. 133, pt. B, No. 2, pp.54-60.
7. Zienkiewicz, O.C. and Cheung, Y.K. (1967). The Finite Element Method in Structural and Continuum Mechanics, McGraw-Hill, London, England,